# Thermal Loading of a Direct Drive Target in Rarefied Gas

B. R. Christensen[1], A. R. Raffray[1] and M. S. Tillack[1]

[1]Mechanical and Aerospace Engineering Department and Center for Energy Research, University of California, San Diego, La Jolla, CA 92093-0438

## Abstract

In an inertial fusion energy (IFE) power plant, each fusion micro-explosion (~10 Hz) causes thermal and structural loads on the IFE reactor wall and driver optics. The loading on the wall must remain sufficiently low to ensure that economic and safety constraints are met.

One proposed method for decreasing the intensity of the wall loading is to fill the reaction chamber with a gas, such as Xe, at low density. The gas will absorb much of the radiation and ion energy from the fusion event, and then slowly release it to the chamber wall. Unfortunately the protective gas introduces major heat loads on the direct drive target. The thermal loading of a target, during injection, largely determines the viability of that target upon reaching chamber center. Thus, the density of the gas must be carefully selected to ensure that a target will survive injection.

The objective of this work is to quantify and characterize the heat flux resulting from the interaction of the target and the protective gas. The loading of the target is modeled using DS2V, a commercial DSMC program. Using DS2V, this work explores the effect of the protective gas density, temperature, sticking (condensation) and accommodation coefficients on the heat flux to the target.

## Introduction

The direct drive fusion concept utilizes multiple laser beams to compress and heat small spherical pellets loaded with fusion fuel, resulting in a fusion micro-explosion. Initial perturbations in the target, caused by surface roughness, vapor bubbles, or other inconsistencies, must be minimized to maximize the implosion efficiency [1-5].

An understanding of the thermal and mechanical response of the target as it travels through a reaction chamber is important since, as heat loading increases the temperature of the target, thermal expansion and phase change could threaten the integrity of the target. To understand and model the thermal and mechanical response of a direct drive target, the thermal loading of the target must first be quantified.

By coupling the thermal loading model with the target response model it will be possible to determine the maximum amount of chamber gas to ensure that a viable target is delivered for implosion. Note that the gas density might also be limited by the ability to place the target accurately and repeatably in the reaction chamber due to the buffeting of the chamber gas. The effect of gas density on target placement is not considered in this study.

It is also essential that the loading on the reaction chamber walls and optics remains sufficiently low to ensure that economic and safety constraints are met. For each fusion micro-explosion (~10 Hz), ions and thermomechanical stresses from heat loads threaten to damage the reactor wall and driver optics. One proposed method for decreasing the intensity of the wall loading is to fill the reactor chamber with a gas, such as Xe, at low density [5]. The gas will absorb much of the radiation and ion energy from the fusion event, and then slowly release it to the chamber wall. Unfortunately, the protective background gas introduces major heat loads on the target due to convection and condensation.

Previous works have investigated convection heat transfer on a direct drive target [6-8]. The condensation of the protective gas on the target is completely neglected in the work by Siegel [7]. Raffray et al [8] account for the release of latent heat with condensation, but the model does not remove "condensed" particles from the flow. In this study the effect of condensation is fully accounted for by considering the release of latent heat, as well as the removal of the condensed particles from the flow.

## Reaction Chamber Environment

Radiation and convection (with condensation) are the thermal loading mechanisms considered in this study. The radiation loading is simply calculated using the Stefan-Boltzman law with the expected reaction chamber wall temperature and the target surface reflectivity. The radiation heat flux is expected to be 0.2 – 1.2 W/cm$^2$.

Xe has been proposed as a good candidate for the protective gas [5]. It is expected that the Xe density will be between 3.22e19 m$^{-3}$ – 3.22e21 m$^{-3}$ (1 – 100 mtorr at 300 K). The range of Knudsen numbers, based on a typical direct drive target (diameter = $d_{Taget}$~ 4mm) in Xe for the above density range, is found to be 0.375 (high-density) to 37.5 (low-density). Therefore, the transition regime applies for the high-density cases and the free molecular regime for the low-density cases.

Since the temperature of the protective gas has not yet been determined, minimum and maximum temperatures of 1300 K and 4000 K are assumed in this study. An additional heat load, not considered in this

paper, would exist if plasma conditions were present in the chamber at the time of injection.

**Modeling Convective Heat Transfer**

Due to the high Knudsen number, for a target in a chamber environment, the convective heat transfer is calculated using DS2V [9] (a commercial DSMC program). The kinetic theory of gases is used to verify the results from DS2V. For a stream of gas traveling toward a semi-infinite transparent plane at the overall velocity $u$, the mass flux (kg/m$^2$-s) is given by kinetic theory as [5]:

$$j = \left(\frac{M}{2\pi R}\right)^{1/2}\left[\Gamma\sigma_c\frac{P_g}{T_g^{1/2}} - \sigma_e\frac{P_f}{T_f^{1/2}}\right] \quad (1)$$

where $M$ (kg/mol) is the molecular weight of the gas, $R$ (J/K-mol) is the universal gas constant, $\sigma_c$ and $\sigma_e$ are the condensation and evaporation coefficients, $P_g$ and $T_g$ are the gas pressure (Pa) and temperature (K), and $P_f$ and $T_f$ are the condensed fluid/solid pressure and temperature. $\Gamma$ is a weighting function based on $u$ and the characteristic molecular velocity of the gas.

For comparison with the DS2V results it is convenient to convert the mass flux (Eq. 1) to number flux by using the equation:

$$f = \frac{j}{M}N_A \quad (2)$$

where $N_A$ is Avagadro's number. The simple kinetic theory, as given by Eq. 1, does not account for interactions between particles that have been reflected from a surface and the incoming stream of particles. In reality, reflected particles will interact with the incoming stream and change the density and temperature of the gas near the surface. The fraction of particles that condense on a surface, after interacting with it, is given by the condensation or sticking coefficient ($\sigma_c$).

The appropriate $\sigma_c$ for Xe at 4000 K interacting with a cryogenic target surface is uncertain. Several studies have been aimed at determining $\sigma_c$ for gases at temperatures < 2500 K, interacting with a cryogenic surface [10,11]. Brown et al [10] give experimental results for several gases with temperatures between 1000 K and 2500 K. The results suggest that there is a critical surface temperature below which the condensation coefficient is near unity, and above which the condensation coefficient decreases rapidly. For each gas considered, the critical surface temperature is much lower than the triple point temperature of the gas.

Arumainayagam et al [12] studied the condensation of Xe on a Pt surface held at 95 K. They found that the probability of a Xe molecule being trapped on the Pt surface, during its *initial* interaction with the surface, decreased dramatically with increasing translational energy of the Xe.

Due to the expected high gas temperature in an IFE reaction chamber, and the considerable uncertainty in the behavior of the condensation coefficient as a function of surface temperature, data for the $\sigma_c$ of Xe at reaction chamber conditions, interacting with a simulated target, are needed.

For each particle that does not condense it is important to know how much of the particle's incident energy is transferred to the surface of the target. The accommodation coefficient ($\alpha$) is the fraction of energy that is transferred to a surface, from a particle, during an interaction between a gas and a surface.

The data for the accommodation coefficient is limited to gases with temperatures of ~ 1400 K, interacting with cryogenic surfaces [13], where $\alpha$ is found to be very near to unity. $\alpha$ is not completely independent of the condensation coefficient, since $\alpha = 1$ for each particle that condenses.

**DS2V Results**

To determine the heat flux on a target, and to investigate the influence of the condensation ($\sigma_c$) and accommodation coefficient ($\alpha$), DS2V was employed. The assumptions used in DS2V for modeling target injection are:

1. Axisymmetric flow around a 4mm diameter sphere (target).
2. Target surface temperature = 18 K = constant.

The coordinate system and placement of the target used in DS2V are shown in fig. 1.

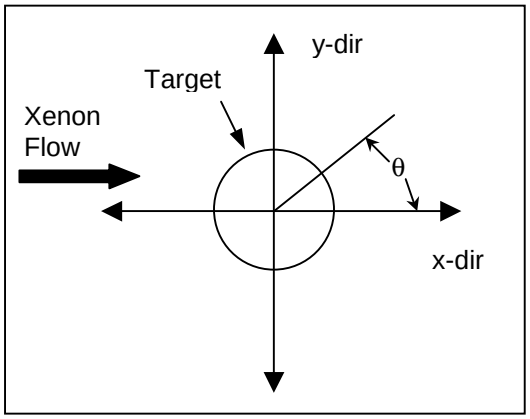


**Figure 1.** The coordinate system, flow direction, and target placement used in DS2V.

Fig. 2 shows the number flux when the Xe density is 3.22e21 m$^{-3}$, the target injection velocity is 400 m/s, and $\alpha$ = 1. Due to symmetry, fig. 2 is plotted for one half of the target as a function of the angle from the trailing edge, where $\theta$ = 0 is the trailing edge of the target, and $\theta = \pi$ is the leading edge. Fig. 2 shows that Eq. 1 and DS2V are in good agreement at the leading edge ($\theta = \pi$) when $\sigma_c$ = 1. At the trailing edge ($\theta$ = 0) with $\sigma_c$ = 1, Eq. 1 predicts a number flux of approximately one-half of the value given by DS2V. The good agreement, between DS2V and Eq. 1, at the leading edge of the target serves to verify the results of

DS2V. The discrepancy at the trailing edge occurs because the kinetic theory results are based on a semi-infinite plane traveling through the gas, which removes particle scattering possibilities that occur when a gas travels around a sphere.

Fig. 2 shows that the number flux *increases* when $\sigma_c$ is decreased from 1 to 0. This increase is a result of the interaction between reflected particles and the incoming stream.

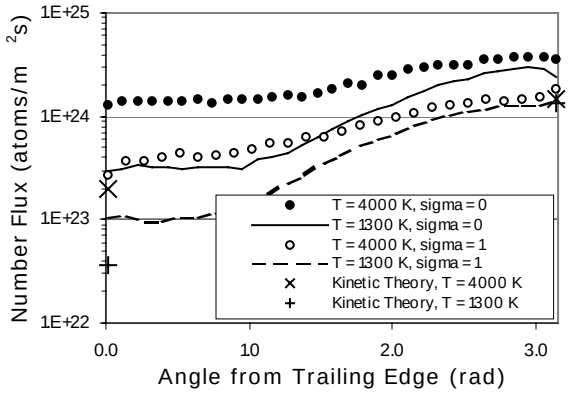


**Figure 2.** The number flux at the target surface for Xe at 3.22e21 $m^{-3}$ is a strong function of $\sigma_c$.

Fig. 3 shows the heat flux when the Xe density is 3.22e21 $m^{-3}$, the target injection velocity is 400 m/s, and $\alpha$ = 1. Notice that increasing $\sigma_c$ from 0 to 1 increases the heat flux by ~2.5 times for the 1300 K case, and ~ 2 times for the 4000 K case. Since the number flux is *decreased* by changing $\sigma_c$ from 0 to 1 (fig. 2), and the heat flux is *increased*, the reflected (uncondensed) particles are apparently "shielding" the target by decreasing the average temperature of the incoming gas stream, thus reducing the heat flux.

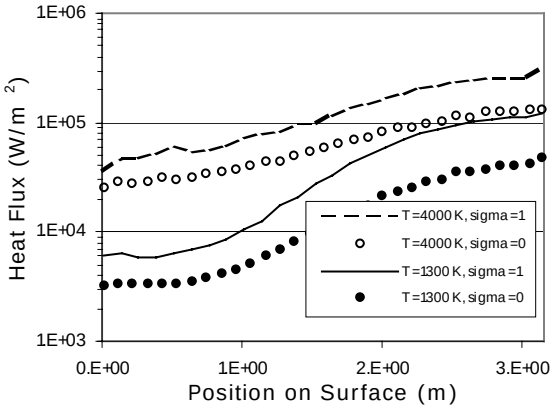


**Figure 3.** The heat flux at the surface of the target for Xe at 3.22e21 $m^{-3}$ is strong function of $\sigma_c$.

The rapid increase in heat flux with θ, seen in fig. 3, suggests that rotating the target about the y- or z-axis (fig. 1) as it traveled through the chamber would reduce the time average maximum heat flux. A summary of the maximum heat flux (at the leading edge), including the radiation heat flux, for several protective gas densities and temperatures are given in Table 1.

Fig. 4 shows the influence of $\sigma_c$ and α on the maximum incident heat flux (leading edge of the target). The injection velocity is set at 400 m/s and the Xe density and temperature are 3.22e21 $m^{-3}$ and 4000 K respectively. The maximum heat flux ($\sigma_c$ = 1, $\alpha$ = 1), by which each case is normalized, is ~ 27 $W/cm^2$. Notice that when $\alpha$ = 1, a significant decrease in the heat flux is not seen until $\sigma_c$ < 0.8. If there were no interaction between reflected and incoming particles, the normalized incident heat flux, when α =1, would be unity for all $\sigma_c$. Thus, the decreasing heat flux with decreasing $\sigma_c$ (fig. 3), when α = 1, is a manifestation of shielding. In general, reducing α causes the heat flux to decrease more rapidly with decreasing $\sigma_c$.

**Table 1.** A Summary of total expected heat flux reported in $W/cm^2$.

| | **n = 3.22e19 $m^{-3}$** | | **n = 3.22e20 $m^{-3}$** | | **N = 3.22e21 $m^{-3}$** | |
|---|---|---|---|---|---|---|
| $\sigma_c$ | Tgas = 1300 K | Tgas = 4000 K | Tgas = 1300 K | Tgas = 4000 K | Tgas = 1300 K | Tgas = 4000 K |
| 0 | 0.3 - 1.3 | 0.4 - 1.4 | 0.9-1.9 | 2.3-3.3 | 4.4 - 5.6 | 14.1 - 15.1 |
| 1 | 0.32 -1.32 | 0.47 - 1.47 | 1.3 - 2.3 | 2.7-3.7 | 11.5 - 15.5 | 27.3 - 28.3 |

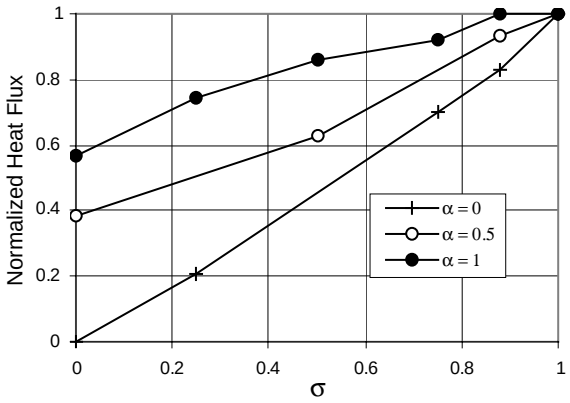


**Figure 4.** The normalized heat flux as a function of $\sigma_c$ and α.

Fig. 5 shows the effect of the injection velocity, Xe density, and $\sigma_c$ on the maximum incident heat flux (at the leading edge of the target). Notice that when $\sigma_c$ = 1 the relationship between the heat flux and the Xe density is linear for each injection velocity. As expected, when $\sigma_c$ = 0 the heat flux is less than when $\sigma_c$ = 1 for all Xe densities. When $\sigma_c$ = 0, the heat flux increases at a slower rate as the Xe density is increased. From these results it is apparent that the shielding effect (described above) occurs over the density and velocity

range studied, and is a stronger effect as the density is increased.

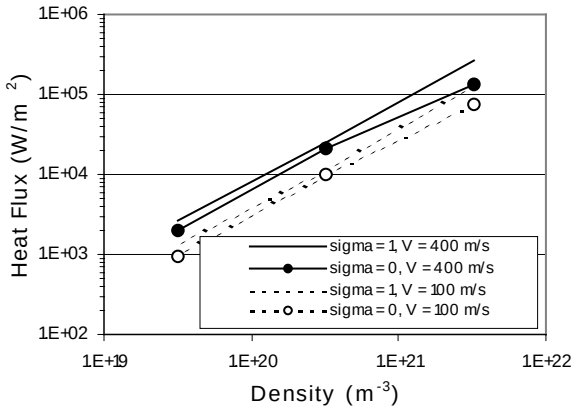


**Figure 5.** The heat flux as a function of protective gas density and injection velocity.

**Maximizing the Protective Gas Density**

The effect of Xe density, target injection velocity, and target design are evaluated by coupling the DS2V results and the results from a numerical model that predicts the response of a direct drive target to an imposed heat flux. In each case it is assumed that the target will fail if the DT temperature exceeds the DT triple point. Through this simple analysis the optimum injection velocity (maximizing Xe density) can be determined.

Fig. 6 shows the maximum allowable Xe density for a basic target (without insulation) for several initial target temperatures, and $\sigma_c$ = 0. For this configuration the maximum density increases with increasing injection velocity. Also notice that decreasing the initial target increases the maximum allowable Xe density significantly.

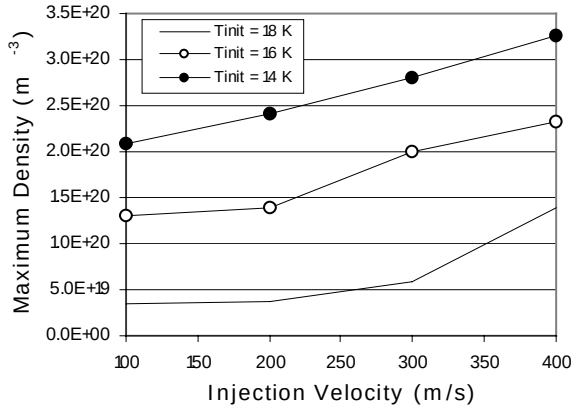


**Figure 6.** The maximum allowable protective gas density based on target survival for a basic target.

Fig. 7 shows the maximum allowable Xe density for a basic target without insulation, where $\sigma_c$ = 1. In this case there is a clear maximum in the allowable Xe density for each initial target temperature. For initial target temperatures of 14 K and 16 K the maximum allowable density occurs at ~ 200 m/s. For an initial target temperature of 18 K the maximum is at an injection velocity of ~ 400 m/s. Thus, for low initial target temperatures it is clearly advantageous to inject the target at 200 m/s if $\sigma_c \sim 1$.

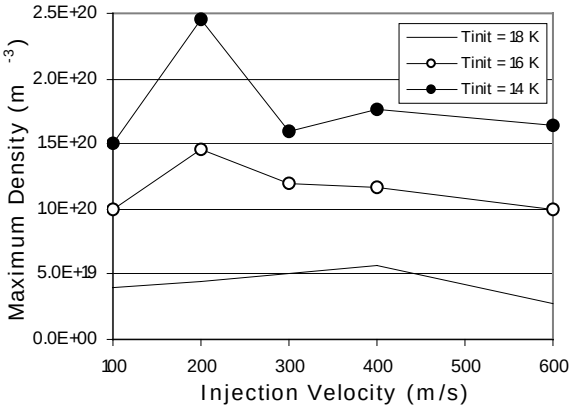


**Figure 7.** The maximum allowable protective gas density based on target survival for a basic target.

Fig. 8 shows the maximum allowable Xe density for a target insulated with 100 μm of 10 % dense porous polystyrene foam, and $\sigma_c$ = 1. For each initial target temperature, the maximum gas density always increases with increasing injection velocity.

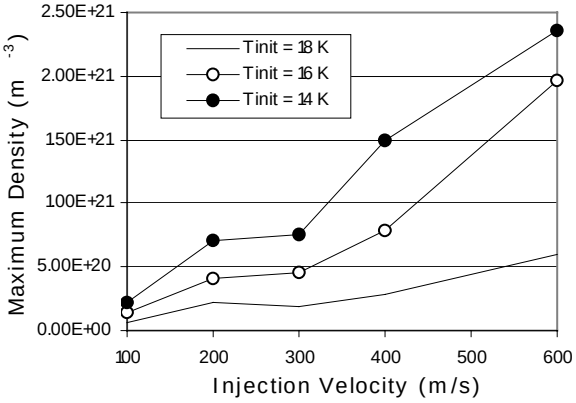


**Figure 8.** The maximum allowable protective gas density based on target survival for a basic target.

As data is obtained for $\sigma_c$ and α, DS2V could be used in conjunction with the target numerical model to optimize the injection velocity for a given target design.

## Conclusions

While the actual environment in an IFE reactor chamber is unknown, it is possible to simulate the chamber environment parametrically to gain a greater understanding of the thermal loading of a direct drive target.

The commercial DSMC program, DS2V, has been shown to accurately model the convective (including condensation) thermal loading of a direct drive target. DS2V allows for the study of the influence of the condensation and accommodation coefficient on the thermal loading of the target.

The condensation coefficient influences both the number and heat flux on the target. The number flux increases with decreasing condensation coefficient, while the heat flux decreases. This decrease in heat flux, with decreasing condensation coefficient, occurs because the particles that are reflected off of the target surface interact with the incoming gas reducing the incident energy of subsequent particles that interact with the surface.

A decrease in the accommodation coefficient also decreases the heat flux for the same condensation coefficient. If the condensation coefficient is found to be > 0.8, the accommodation coefficient would have to be <= 0.5 for a 10% or greater decrease in incident heat flux.

The maximum allowable protective gas density is a function of injection velocity, target design, and condensation coefficient. When the condensation coefficient is unity, the maximum protective gas density increases with increasing injection velocity. The injection velocity may be optimized to obtain the maximum amount of protective gas for a given target design.

The gas density may also be limited by the ability to accurately and repeatably place the target at the intended implosion point. The effect of condensed background gas on the surface roughness and reflectivity of the target should also be investigated in the future.

## References


1. R. Cook, “Creating Microsphere Targets for Inertial Confinement Fusion Experiments,” Energy and Technology Review, April 1995.
2. J. Grun, et al., “Rayleigh-Taylor Instability Growth Rates in Targets Accelerated with a Laser Beam Smoothed by Induced Spatial Incoherences,” Phys. Rev. Lett. 58(25), June 1987, pp. 2672-2676.
3. C. J. Pawley, et al., “Observation of Rayleigh-Taylor growth to short wavelengths on NIKE,” Phys. Plasmas, 6(2), February 1999, pp. 565-570.
4. J. P. Knauer, et al., “Single-mode, Rayleigh-Taylor growth-rate measurements on the OMEGA laser system,” Phys. Plasmas, 7(1), January 2000.
5. A. R. Raffray, et al., “IFE chamber walls: requirements, design options, and synergy with MFE plasma facing components,” Journal of Nuclear Materials, 313-316 (2003), pp. 23-31.
6. R. W. Petzoldt, et al, “Direct drive target survival during injection in an inertial fusion energy power plant,” Nucl. Fusion, Vol. 42, pp. 1351-1356, 2002.
7. N. P. Siegel, “Thermal Analysis of Inertial Fusion Energy Targets,” Master of Science Thesis, San Diego State University, May 2000.
8. A. R. Raffray, J. Pulsifer, M. S. Tillack, “Target Thermal Response to Gas Interactions,” UCSD Technical Report, UCSD-ENG-092, http://aries.ucsd.edu/FERP/reports.shtml.
9. DS2V Version 2.1, GAB Consulting.
10. R. F. Brown, D. M. Trayer, and M. R. Busby, “Condensation of 300 – 2500 K Gases on Surfaces at Cryogenic Temperatures,” The Journal of Vacuum Science and Technology, Vol. 7, No. 1, 1969.
11. J. P. Dawson, and J. D. Haygood, “ Cryopumping,” Cryogenics, Vol. 5, No. 2, April 1965.
12. C. R. Arumainayagam, et. al., “Adsorbate-assisted adsorption: Trapping dynamics of Xe on Pt(111) at nonzero coverages,” Journal of Chemical Physics, Vol. 97, No. 7, October 1991.
13. W. Frost, *Heat Transfer at Low Temperatures*, Plenum Press, New York, 1975.